Brazilian Journal
of Chemical
Engineering

ISSN 0104-6632
Printed in Brazil
www.abeq.org.br/bjche

Vol. 33, No. 03, pp. 525 - 540, July - September, 2016
dx.doi.org/10.1590/0104-6632.20160333s20150125

LARGE EDDY SIMULATION COMBINED WITH EQUIVALENT DIAMETER FOR TURBULENT JET MODELLING AND GAS DISPERSION

E. S. Ferreira Jr. and S. S. V. Vianna*

Universidade Estadual de Campinas (UNICAMP), Faculdade de Engenharia Química, Campinas - SP, Brazil
Phone: (55) (19) 3521-3947
*E-mail: savio@feq.unicamp.br; savio.vianna@cantab.net
E-mail: elmo@feq.unicamp.br

(Submitted: February 26, 2015 ; Revised: June 23, 2015 ; Accepted: June 23, 2015)

Abstract - CFD modelling combines transport phenomena and numerical approaches to solve physical problems. Although numerical modelling of flow scenarios is the cutting edge of flow modelling, there seems to be room for improvement. This paper proposes an approach for jet modelling in a low Mach number computational code. The methodology is based on the equivalent diameter and velocity profile calculated downstream from the jet leak orifice. The novel model DESQr (Diameter of Equivalent Simulation for Quicker Run) is combined with LES (Large Eddy Simulation) to calculate the gas jet profile due to accidental releases. The model is implemented in the framework of FDS (Fire Dynamics Simulator) and the open source code is modified to handle gas dispersion scenarios. Numerical findings for jet modelling and gas dispersion are compared with experimental data. The results are also compared with a commercial CFD tool. Good agreement is observed. Significant computational time reduction is achieved. A free open source CFD tool emerges and the results presented in this work are promising.
Keywords: LES; CFD; Turbulent jet; Gas dispersion; Process safety.

INTRODUCTION

Computational Fluid Dynamics (CFD) has more recently been applied in various industrial scenarios. The chemical industry, in particular, has major interest in flow modelling as it is of crucial importance in all stages of design.

The computational time is an important point to be considered in any CFD case. More recently the utilisation of LES (Large Eddy Simulation) and RANS (Reynolds Averaged Navier-Stokes) approach has played an important role in engineering. The benefits of the former outweigh the computational time when RANS cannot provide reliable results, particularly when significant gradients are present (Derjon *et al*., 2007).

Having said that, LES is computationally expensive for the industry standards where quick responses are demanded. Therefore, most of the applications of LES are somehow limited to the academic environment.

The current research is focused on the modification of the low momentum LES code (namely FDS - Fire Dynamic Simulator) in order to deal with jet scenarios in an accurate manner and faster than traditional approaches. A novel jet model DESQr (Diameter of Equivalent Simulation for Quicker Run) is proposed. The model calculates a new set of boundary conditions based on stagnation values in the pipeline and its findings are coded into FDS. The model is not limited to FDS, but it is also entitled to be used in any CFD code. Findings from DESQr-FDS

*To whom correspondence should be addressed
This is an extended version of the work presented at the 20th Brazilian Congress of Chemical Engineering, COBEQ-2014, Florianópolis, Brazil.

are compared with experimental data and ANSYS-CFX code. Good agreement is observed with significant computational time reduction when DESQr is applied in the jet transition zone.

The current paper covers the various aspects of turbulent jet modelling and gas dispersion modelling in the next section. The main advances in the field of numerical modelling are also presented and the research gaps which deserve special attention and that offer room for improvement are introduced.

The mathematical background for the proposed DESQr model is discussed. The basic equations for isentropic releases are presented and the model development is discussed in accordance with the ideas suggested by Benintendi (2010).

Then, the numerical findings from DESQr-FDS are addressed and an extensive discussion concerning jet modelling is presented. The numerical results are compared with experimental data and also with a commercial CFD tool. Subsequent Sections are dedicated to improvements obtained concerning the computational time and to the discussions of the gas dispersion simulation and the wind analysis. There is a comprehensive analysis of the code developed and the results are once again compared with a commercial CFD tool. The cases resolved using the commercial CFD tool applied the RANS approach as it is the first choice in the industry. The last Section summarises the research work and explores new avenues for future work.

NUMERICAL MODELLING OF TURBULENT JETS AND GAS DISPERSION

Jet flows have many applications and are of relevant importance in drying processes, heating and ventilation, gas discharge and gas dispersion and various others aspects of engineering. More recently, Wakes (2003) investigated the influence of different shapes of leak holes and how they impact the near region of a gas jet. The impact on gas dispersion, as suggested by Wakes (2003), could be significant whether the jet is considered axisymmetric or is treated as having a high aspect ratio. Another important aspect of gas dispersion is the presence of large obstacles and buildings, which are a common feature in chemical process areas. In this case, the utilisation of Gaussian models is limited and more advanced tools, such as CFD (Computational Fluid Dynamics) is preferable. It is not rare that the impact of complex geometries on the gas flow and the wind pattern is assessed using simpler models and CFD techniques (Tauseef *et al*., 2011) in order to verify the differences in the results.

The behaviour of a dense gas cloud is also a subject of interest, particularly when LPG (Liquified Petroleum Gas) is considered (Scargiali *et al*., 2005). The area of research is not limited to flammable gas, but there seems to be an increasing interest in carbon dioxide release (Witlox *et al*., 2014) as well as other toxics gases, such as ammonia (Galeev *et al*., 2013).

Although the modelling of gas dispersion is very important, there are no significant applications of open source CFD tools to accidental dispersion problems. Most of the time commercial tools are used as there is limited documentation and technical support for open source codes. The application of FDS (Fire Dynamics Simulator) for dispersion scenarios was first suggested by Mouilleau *et al*. (2009). However the case investigated by Mouilleau *et al*. (2009) does not present any modification in the code. It relies on the conservation of a scalar switching off the combustion. Due to numerical instability of the tool, the gas dispersion scenario is calculated when the transport of the flammable cloud is governed by diffusion and, consequently, very low momentum is considered.

It turns out, however, that, prior to gas dispersion, a leak in the process pipe or vessel must occur. As a consequence, a turbulent jet will arise. Jet flows from rupture are caused by a pressure drop through an orifice and vary greatly depending upon the upstream flow characteristics (stagnation conditions before leakage) and the rupture shape (Wakes, 2003). Most of the interactions and mixing between the ambient and jet fluids take place in a shear layer. In a turbulent jet, the air entrainment and momentum transfer originate in this layer. Thus, the fluid within the jet is decelerated and the fluid surrounding the jet is accelerated. As a consequence, the jet increases its radius (spreading) and its mass rate.

The turbulent jet can be characterized by the presence of three specific well known regions, defined by the downstream jet centreline velocity (Hussain and Zamman, 1981). These regions are: potential core region, convergence zone where the jet centreline velocity is equal to the exit velocity of the nozzle. The potential core region often extends up to 4 times the exit diameter (4De) to 6.5 times the exit diameter (6.5De), depending on the velocity profiles and the turbulence levels at the nozzle exit; transition region, where the jet is strongly mixed with ambient air and the shear layer emerges, increasing the turbulent flow fluctuation. Therefore the jet centreline velocity starts to decay rapidly. This region usually extends up to 6.5De to 20De; and a self-similar region, in this region the centreline velocity profile is similar and the velocity decay is smooth (Hussain and Zamman, 1981). The model proposed in this work is focused on the

potential core region of the jet. The transition and the self-similar regions are modelled numerically in the computational mesh, as will be discussed in the following sections.

FDS – Fire Dynamics Simulator

Fire Dynamics Simulator (FDS) is a free Computational Fluid Dynamics (CFD) code developed by the National Institute of Standards and Technology (NIST). It is based on Direct Numerical Simulation (DNS) and Large Eddy Simulation (LES) methodology to capture the turbulence phenomenon (Mcgrattan *et al*., 2014). In the present research, the LES approach has been used. The available sub-grid models in FDS are constant Smagorinsky, dynamic Smagorinsky and Deardorff models. FDS code has been modified in the context of this work in order to deal with jet modelling. It is important to bear in mind that the code was originally designed for low speed flow cases and therefore it cannot handle high speed gas releases. The original formulation resolves the generalized transport Equation (1), in which ϕ represents the dependent variable (velocity, energy and mass fraction). FDS is explicit, second order accurate and the computational mesh is structured. Turbulence is closed in accordance with the eddy viscosity concept for subgrid modelling.

$$\frac{\partial(\rho\emptyset)}{\partial t} + \nabla(\rho\emptyset\vec{v}) = \beta\nabla^2\emptyset + S_\emptyset \tag{1}$$

The version of the code developed in this work, namely, DESQr – FDS, handles a turbulent jet based on the DESQr model. The code has also been extended to calculate the flammable cloud volume. A detailed description of the DESQr model is presented in the following section.

DIAMETER OF EQUIVALENT SIMULATION FOR QUICK RUN - DESQr

The DESQr model was developed in order to allow for the solution of high speed releases in the framework of numerical computational codes developed for low Mach flows.

The main concept proposed by the DESQr formulation relies on new boundary conditions based on isentropic jet release. Given the initial conditions of the jet (at the exit of the leak orifice) the model is applied to calculate the jet characteristics at a selected distance downstream from the jet orifice.

Figure 1 shows the flowchart of the calculation procedure to obtain the jet exit conditions and the modelled diameter for a specific Mach number in which the flow is no longer influenced by the compressibility effects. The current procedure was adapted from Benintendi (2010), who proposed a model for gas volume calculation for hazardous area classification.

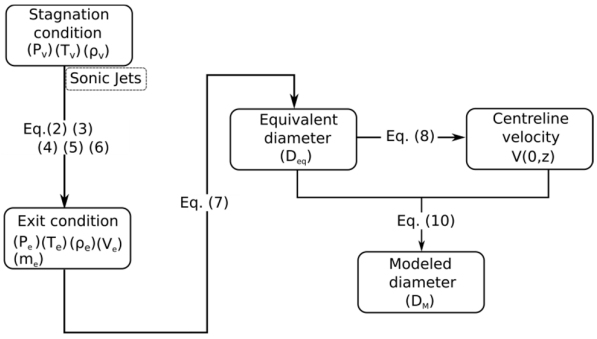

Figure 1: Calculation procedure to obtain the jet exit condition and the diameter downstream from the jet orifice. Adapted from Benintendi (2010).

From Figure 1 it follows that the gas stagnation conditions are used to calculate the exit conditions at the leak orifice using Equations (2) to (5) for sonic flow. Mannan (2012) shows relations for sonic jets. Based on the exit conditions, the equivalent diameter and the downstream jet velocity are calculated by Equations (7) and (8), respectively.

$$\frac{P_e}{P_v} \geq \left(\frac{2}{\gamma+1}\right)^{\frac{\gamma}{\gamma-1}} \tag{2}$$

$$\frac{T_e}{T_v} \geq \left(\frac{2}{\gamma+1}\right) \tag{3}$$

$$\frac{\rho_e}{\rho_v} \geq \left(\frac{2}{\gamma+1}\right)^{\frac{1}{\gamma-1}} \tag{4}$$

$$v_e = \left(\frac{2\cdot\gamma}{\gamma+1} RT_v\right)^{\frac{1}{2}} \tag{5}$$

All exit properties depend on the upstream conditions and the specific heat at constant pressure and at constant volume.

The exit mass flow rate can be calculated by

$$m_e = \rho_e V_e \left(\frac{\pi D_e^2}{4}\right) \tag{6}$$

From Equation (7), the equivalent diameter discussed by Birch *et al*. (1984) is applied in Equation (8) reported by Benintendi (2010).

$$D_{eq} = D_e\sqrt{\frac{P_e}{P_a}} \tag{7}$$

$$V(0,z) = 6\frac{D_{eq}V_e}{z} \tag{8}$$

The downstream velocity $(V(0,z))$ is calculated using the equivalent diameter (D_{eq}), exit velocity (V_e) and the downstream distance (z).

Equation (8) must be used with care. The downstream distance must be greater than the equivalent diameter times six due to the mathematical constraint imposed by Equation (9).

$$z = 6 \cdot D_{eq} \tag{9}$$

Applying the findings from Equations (6), (7), (8) and (9) into Equation (10), the modelled diameter is obtained as follows;

$$D_M = 2\sqrt{2}\cdot 0.082 \cdot z\sqrt{-ln\left(1-\frac{m_e C_e}{2\pi\cdot\rho_a v(0,z) D_{eq} z\cdot 0.082^2}\right)} \tag{10}$$

where C_e stands for the air entrainment coefficient. A detailed description of the mathematical model can be obtained elsewhere, (Benintendi, 2010, 2011).

Ricou *et al*. (1961) recommend that the air entrainment coefficient must be set between 0.20 and 0.32. A discussion about the air entrainment coefficient value for the proposed DESQr model will be presented in a separate section below.

Figure 2 presents the detailed modelling of DESQr applied to a jet case in which the stagnation conditions were used to calculate the new set of boundary conditions represented by the red circle.

The current modified version of the code relies on the DESQr model to calculate the new set of boundary conditions based on the discussion above. The code reads the operational conditions of the vessel or pipeline and uses the new input to calculate the new jet velocity and equivalent diameter. These values are used in the leak name list in order to trigger the jet release.

TURBULENT JET CASE

Simulation and Experiment Set Up

In order to verify the model previously discussed, an investigation of turbulent jet velocity behaviour was performed. The new set of boundary conditions was calculated for the jet release scenario based on the DESQr model (previously discussed). In the numerical model the jet was divided in two regions. The region closer to the leak hole (sonic region of the jet) was modelled while the region downstream from the sonic region was resolved numerically in the CFD code.

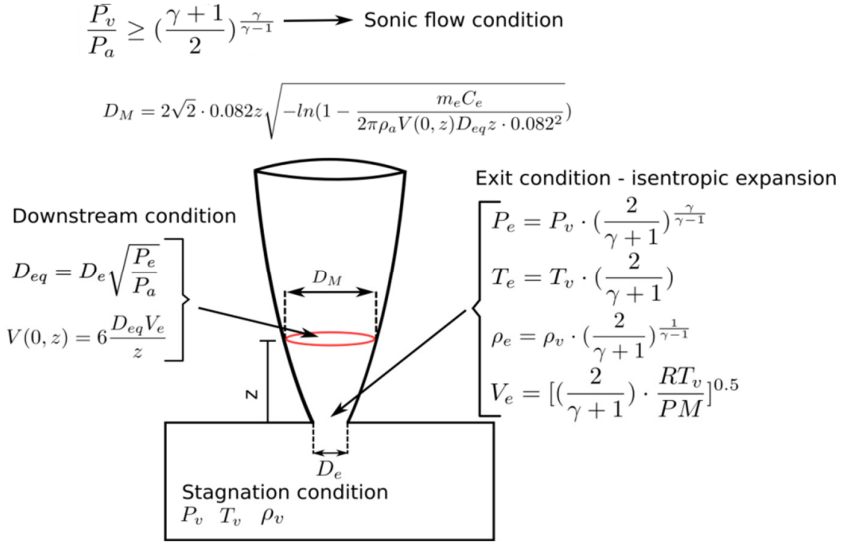

Figure 2: Detailed scheme of the methodology employed for implementation of DESQr in a sonic jet.

The analysis reproduced the experiment conducted by Birch *et al*. (1987) in which an air jet through an orifice (D_e) of 2.7 mm and 340 m/s exit velocity (V_e) was performed in a box 20 mm in length, 20 mm in width and 500 mm in height. Figure 3(a) shows the sketch of the jet pattern observed by Birch *et al*. (1987). Figure 3(b) illustrates the modelled region proposed in this work and the region simulated by the numerical code. Three distances downstream from the jet orifice (*z* distance from Figure 2 were considered (53 mm, 100 mm and 150 mm). Thus, the new boundary conditions, namely the modelled jet orifice D_M, and the downstream velocity, $V(0,z)$, were considered in the numerical simulation.

The simulations comprising 0.025 million cells were been performed on a 3.40 GHz core i7 computer with 8 GB of RAM.

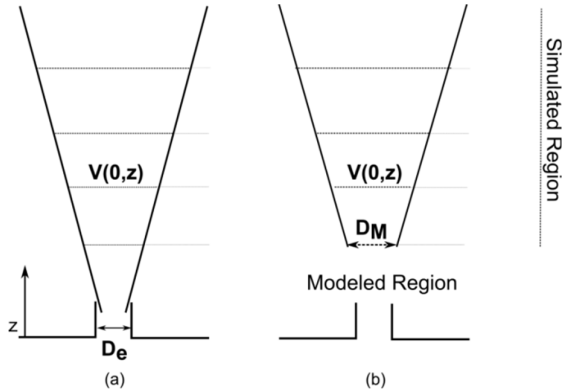

Figure 3: Typical free jet flow obtained in the experiment conducted by Birch *et al*. (1987). (a) Experimental jet setup. (b) Modelled region and the simulated region.

Impact of the Subgrid-Models

Large Eddy Simulation (LES) requires an appropriate choice of the turbulence sub-grid model. Adequate selection of the sub-grid model ensures proper modelling of the eddy viscosity and its associated dissipative effects (Germano *et al*., 1991). Results presented in Figure 4(a) and Figure 4(b) show the jet modelling 53 mm downstream from the jet orifice using the constant Smagorinsky and Deardorff sub-grid models. Figure 4 shows the non-dimensional jet velocity on the y-axis and the non-dimensional distance on the x-axis. The jet velocity is normalised with the sonic velocity at the exit of the leak hole. The distance is normalised with the leak orifice diameter. Experimental data are represented by black dots. Numerical results calculated with the code developed in the framework of FDS are represented by red dot. The solid blue line shows the jet velocity decay simulated with ANSYS-CFX. Analysis of Figure 4(a) shows good agreement between the experimental data and the proposed model for regions closer to the leak orifice. As the distance from the leak orifice increases, the good agreement between the proposed model and experiment is reduced. On the other hand ANSYS CFX (based on RANS – Reynolds Averaged Navier Stokes approach) exhibits good agreement with experimental data.

Figure 4(b) presents the results obtained when the Deardorff model replaced the constant Smagorinsky approach. Analysis of Figure 4(b) shows good agreement between the numerical findings and experimental data for both cases (in-house code and ANSYS CFX). The numerical results presented in Figure 4(a) were calculated with the Smagorinsky constant set to $C_s = 0.2$. The Deardorff model constant value was set to $C_v = 0.1$. In all cases the constant of the sub-grid model were kept at a fixed value.

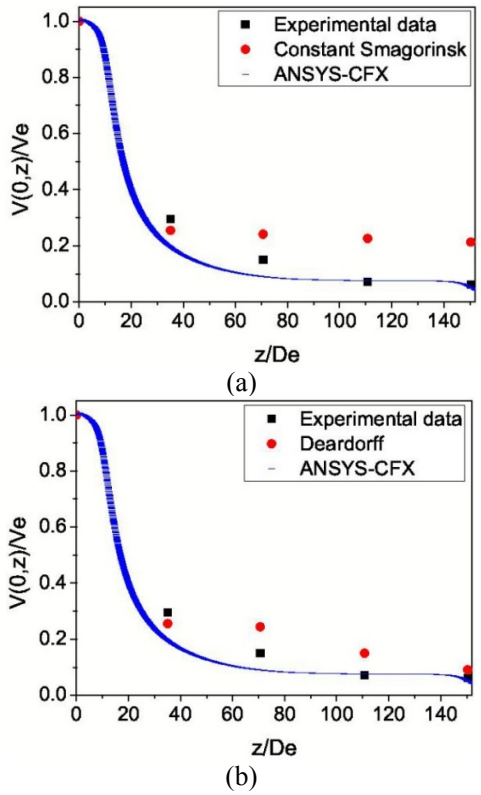

Figure 4: Modelling in FDS 53 mm downstream from the jet orifice using (a) constant Smagorinsky sub-grid model (b) Deardorff sub-grid model. Experimental data (Birch *et al*., 1987).

Although the Deardorff approach presented better results than the Smagorinsky model, there seems to be a significant difference between the numerical findings and the experimental data as far as the RANS

approach is considered. One of the limitations of LES modelling is due to wall effects and the need for a very refined mesh in regions close to the surfaces. One of the improvements put forward by Gemano *et al.* (1991) is the utilisation of a dynamic model in which C_s is allowed to be a function of position and time.

Figure 5 below presents the same simulation previously discussed in Figure 4. Analysis of Figure 5 shows significant improvement in the results when the dynamic model is considered.

Based on the improvement obtained with the utilisation of the dynamic Smagorinsky model, the following sections as well as the gas dispersion modelling, adopted the dynamic approach for C_s .

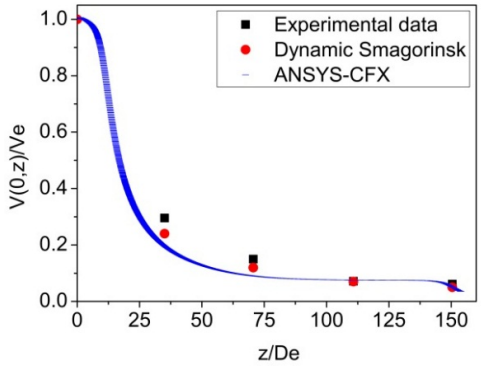

Figure 5: Modelling in DESQr-FDS 53 mm downstream from the jet orifice using the dynamic Smagorinsky sub-grid model. Experimental data (Birch *et al.*, 1987).

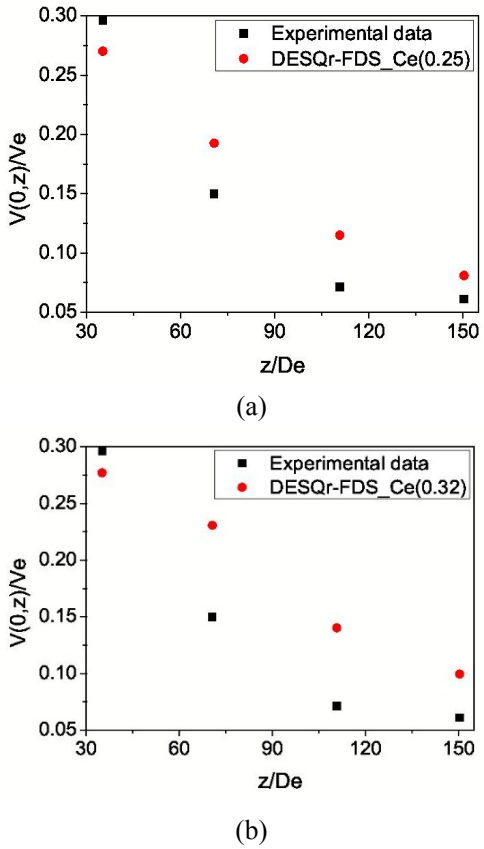

Figure 6: Modelling in FDS 53 mm downstream from the jet orifice using. (a) Entrainment coefficient constant set to 0.25 (b) and entrainment coefficient set to 0.32. Experimental data (Birch *et al.*, 1987).

Impact of the Entrainment Coefficient

The constant values of the entrainment coefficient (C_e) suggested by Ricou and Spalding (1961) were investigated since it plays an important role in the prediction of the modelled diameter (D_M) downstream from the jet orifice. The findings from this analysis are presented in Figure 6. Analysis of Figure 6(a) shows that the results calculated when the air entrainment coefficient was set to 0.25 were better than the numerical results obtained when the constant was set to 0.32 (Figure 6 (b)).

DESQr Final Set Up

Based on the previous analysis it was possible to come up with the best simulation setup. The air entrainment coefficient was set to 0.20. The dynamic Smagorinsky sub-grid model replaced the fixed constant approach, allowing C_s to be a function of time and space.

Figure 7 compares the centreline velocity decay for the modelling proposed with experimental data (Birch *et al.*, 1987) and ANSYS-CFX. Analysis of the plots shows a similar velocity profile. The ANSYS-CFX simulation was performed by Ferreira *et al.* (2014). The modified FDS code based on the DESQr formulation calculated the velocity profile applying the set of boundary conditions for three distances downstream from the leak orifice, 53 mm, 100 mm or 150 mm, respectively. Figure 7 also presents the velocity at the exit of the orifice as well as at the coupling distance. The coupling distance must be understood as the point where the proposed model couples with the numerical analysis. It may also be thought of as the new boundary condition for the numerical simulation.

Analysis of Figure 7(a), (b) and (c) shows very good agreement between numerical findings and experimental data. It important to note that, although the distance from the leak orifice increased, the level of agreement remained very similar.

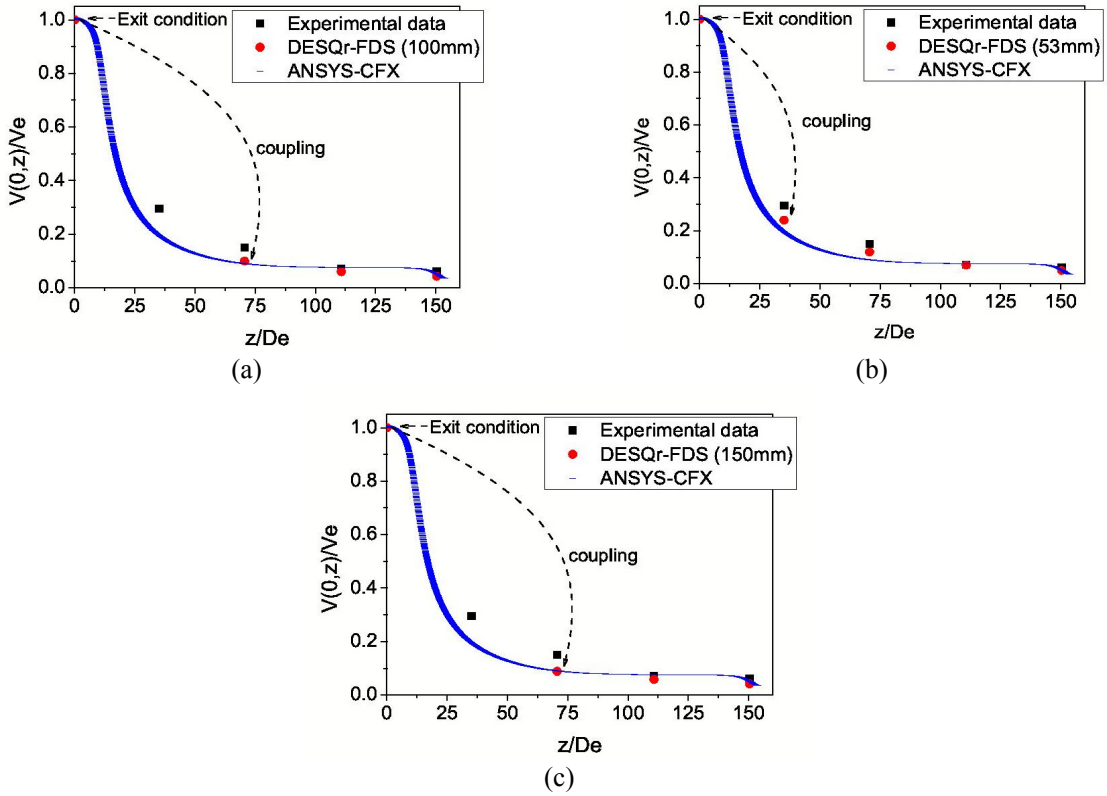

Figure 7: Modelling of the velocity profile using DESQr-FDS. Results are compared with ANSYS-CFX and experimental data (Birch *et al*., 1987) (a) 53mm downstream from the jet orifice. (b) 100mm downstream from the jet orifice. (c) 150mm downstream from the jet orifice.

The following section discusses the impact of the new set of boundary conditions on the required computational time.

COMPUTATIONAL TIME REDUCTION DUE TO DESQR

One of the new boundary conditions is the velocity, which becomes lower as it get farther from the jet leak. Based on the CFL condition, the computational time was compared for the three new boundary conditions placed at 53 mm, 100 mm and 150 mm downstream from the jet orifice, using a mesh size of 2.5 mm in all cases. Figure 8 shows the simulation of the turbulent jet and its associated computational time. The jet release scenarios are exactly the same. However, they have been modelled differently. Figure 8(a) shows the velocity plot for the new set of boundary conditions placed at 53mm downstream from the jet orifice. Figure 8(b) and (c) show the same case in which the new set of boundary conditions were placed at 100 mm and 150 mm downstream from the jet orifice, respectively. Analysis of Figure 8(a) shows that the simulation took about 60 hours (computer time) to calculate 3.0 seconds (physical time) of the jet release. Figure 8(b) and (c) shows that the time required by the same physical problem was reduced to around 15 and 12 hours respectively.

Figure 9 shows the level of agreement between DESQr - FDS results (53 mm, 100 mm and 150 mm) and experimental data (from Figure 6) as a function of elapsed computational time. The boundary condition set at 53 mm downstream from the leak orifice gives better agreement with experimental data, when compared with the other sets of boundary conditions (100 mm and 150 mm). On the other hand, it demands a reasonable amount of time to compute the same case, with no significant gain in accuracy.

Based on the findings presented so far, the best computational setup was applied to investigate the gas dispersion scenario modelling. Results are compared with ANSYS-CFX.

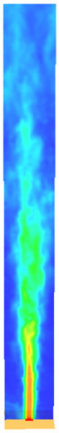

Mesh sizes: 2.5 mm
V = 95 m/s
Time step $_{min}$ = 2.0E-5s
D_M = 9 mm

case (53 mm downstream)

(a)

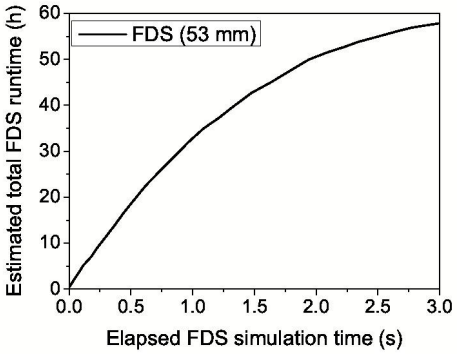

(b)

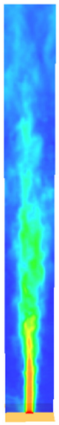

Mesh sizes: 2.5 mm
V = 57.48 m/s
Time step $_{min}$ = 4.0E-5s
D_M = 15 mm

case (100 mm downstream)

(c)

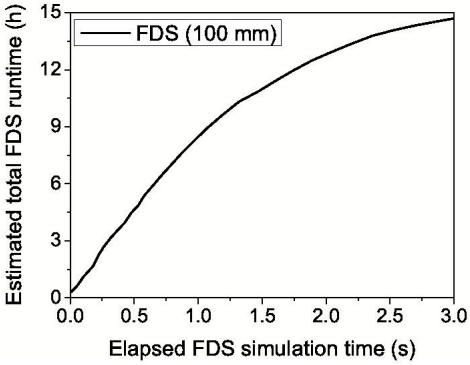

(d)

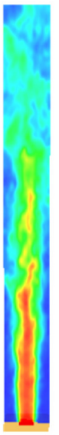

Mesh sizes: 2.5 mm
V = 41.5 m/s
Time step $_{min}$ = 0.93E-4s
D_M = 20 mm

case (150 mm downstream)

(e)

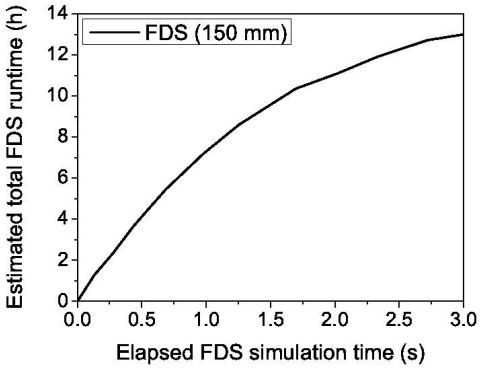

(f)

Figure 8: Simulation of the turbulent jet downstream from the jet orifice and its respective simulation duration for three sets of boundary conditions. (a) 53 mm modelling. (b) 100 mm modelling. (c) 150 mm modelling.

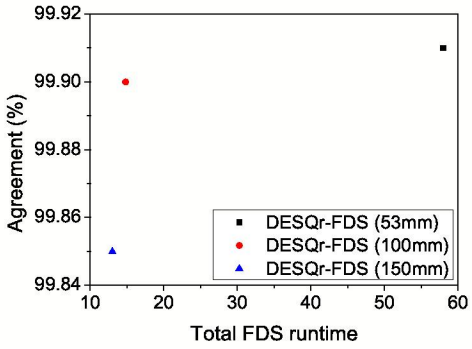

Figure 9: Level of agreement for various equivalent diameters considering in the sensitivity analysis of the DESQr model. Results are compared with experimental data. Accuracy is reduced by 0.08% while computational time is reduced 6 times.

THE GAS DISPERSION CASE

Wind Analysis

In order to perform the gas dispersion simulation, a preliminary wind analysis was conducted. This is a very important aspect of the simulation as the dilution of the flammable cloud is governed by the mixing of gas with air.

A clear picture of the pattern of the wind in the process module was obtained by placing monitor points distributed on the process deck. The wind speed in the area was calculated and stored at the set of monitor points presented in Figure 10.

The wind profile at the boundary of the computational domain was set as 2.0 m/s. The wind profile was analysed in a qualitative manner as well as in a quantitative approach.

Figure 11 shows the wind vectors for different instants of time. Analysis of Figure 11 shows that 35 seconds from the beginning of the simulation were required until the wind profile was well established in the deck area.

Based on the discussion above, the gas leak was set to start at 45 seconds in accordance with the steady state behaviour of the wind field in the process area.

Figure 12 calls attention to the wind profile in the area. Figure 12(b) shows much less oscillation as the monitor point is placed just outside the process area. Therefore, the oscillations are much less evident and they are limited to the fluctuations of the velocity around the filtered velocity in the LES modelling.

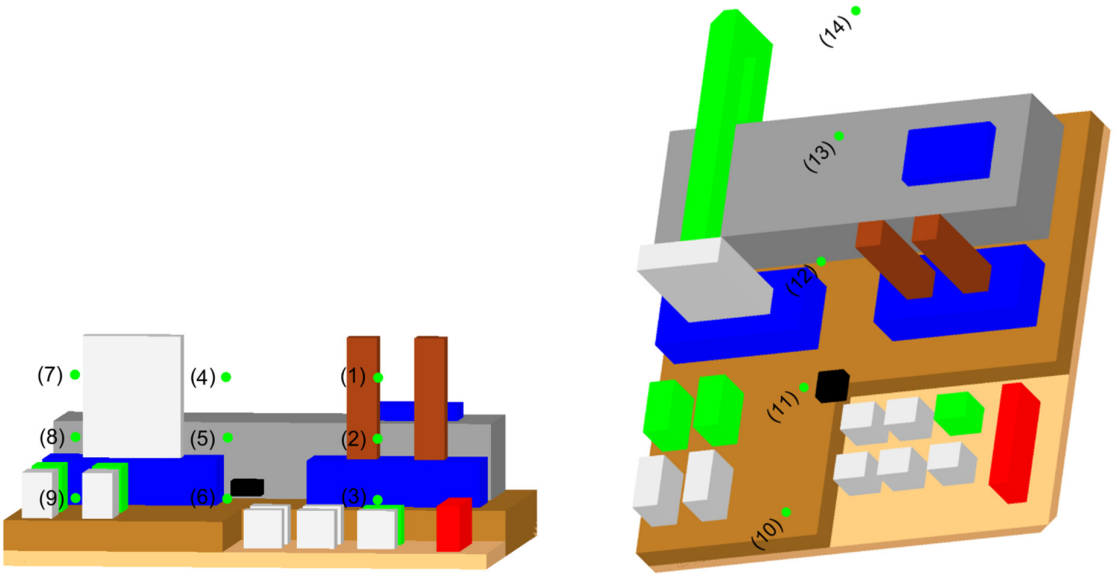

(a) (b)

Figure 10: Wind velocity monitoring points distributed on the platform deck.

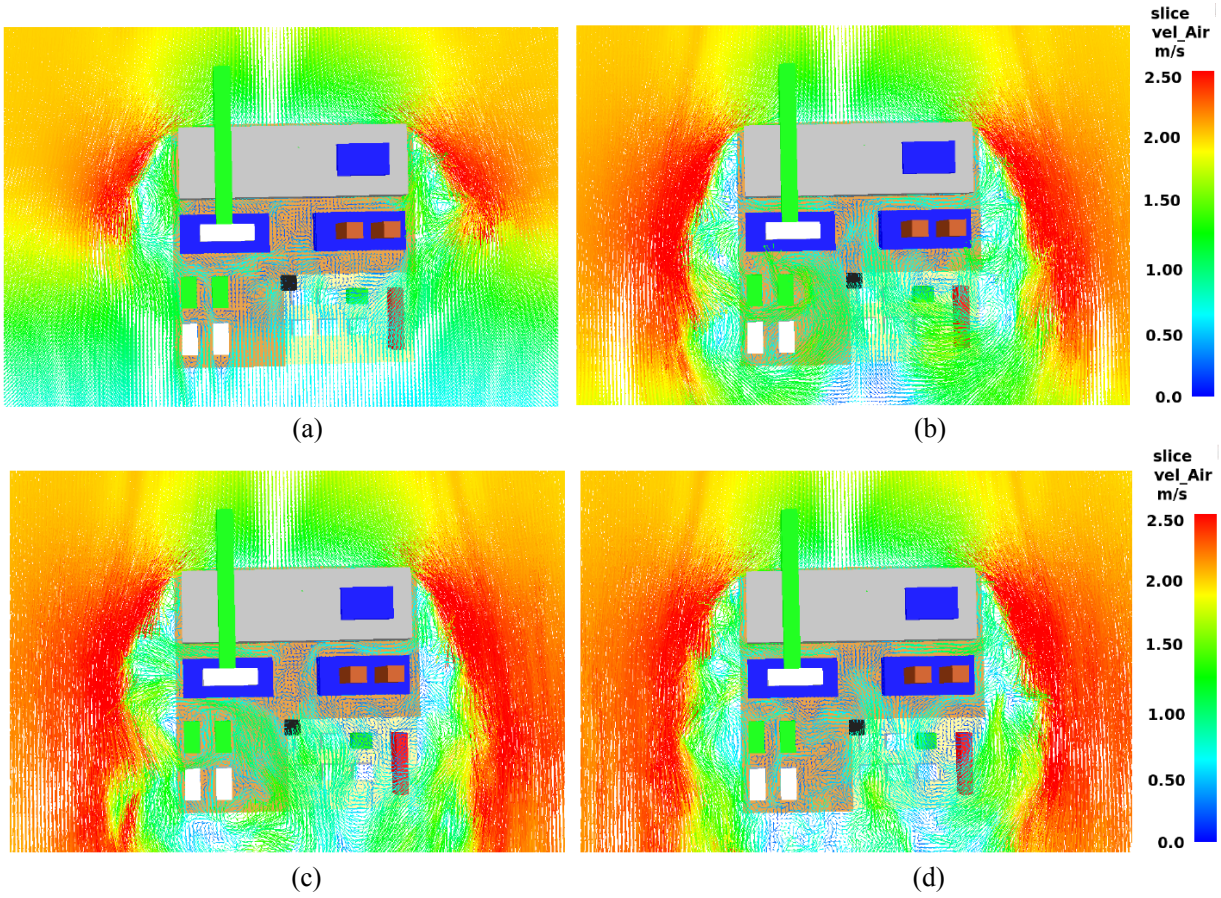

Figure 11: Wind velocity development visualized using vector slices in a plant 2.5 m above the main deck. (a) 15 s of simulation. (b) 25 s of simulation. (c) 35 s of simulation. (d) 45 s of simulation.

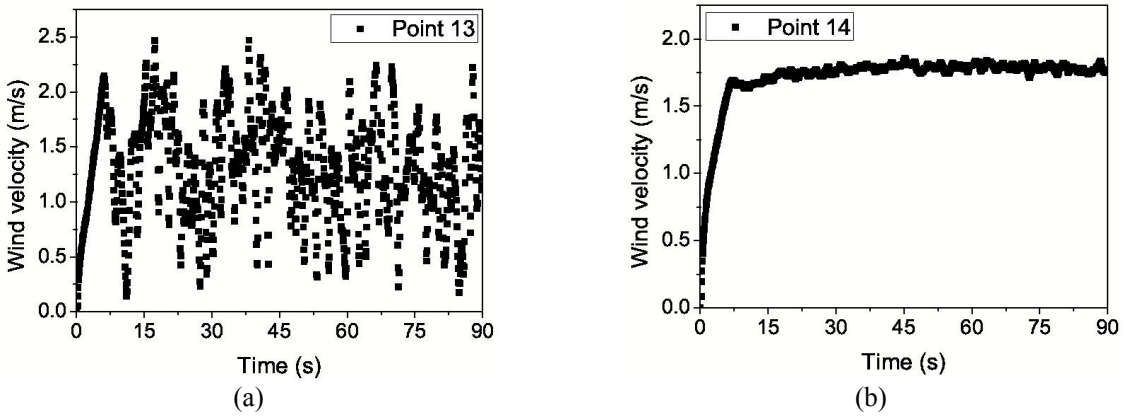

Figure 12: Wind velocity profile captured by the monitoring points. (a) Point 13 and (b) point 14 (point 5 m in height over the deck).

Computational Domain and Mesh

Prior to proceeding to the analysis of gas dispersion, a detailed investigation of the computational domain and mesh size was performed is shown in Figure 13.

Therefore, five distinct computational domains of rectangular shape were considered. The domains for the analysis were selected in accordance with the dimensions of the area to be investigated. Based on the characteristic length scale of the process area, the following computational domains were set up.

- 50.0 m long x 50.0 m wide x 40.0 m in height
- 60.0 m long x 60.0 m wide x 40.0 m in height
- 80.0 m long x 80.0 m wide x 40.0 m in height
- 85.0 m long x 85.0 m wide x 40.0 m in height
- 80.0 m long x 80.0 m wide x 50.0 m in height

The meshing process ensured a refined mesh size, particularly near solid surfaces. The smallest grid size was set to be 25 cm. It is important to bear in mind that the mesh refinement in LES does not necessary ensure grid independency. In fact, the more one refines the mesh the more details of the smaller length scales of the turbulence are resolved in the computational mesh rather than in the sub-grid model.

Therefore, an investigation of the mass of gas released was performed varying the mesh size. The computational mesh size selection was based on the length scale of the main flow and the turbulent kinetic energy spectrum in which most of the wave numbers were captured in the grid.

Analysis of the flammable mass released for the various computational domain sizes selected is shown in Figure 14. Analysis of the plot shows a significant difference in the mass released. The difference between the mass obtained for the largest computational domain and the smallest computational domain is around 42%.

Bearing in mind the findings presented in Figure 14, the smallest computational domain was increased by 5 metres and by 10 metres in order to reduce the effect of the boundaries in the inner computational area.

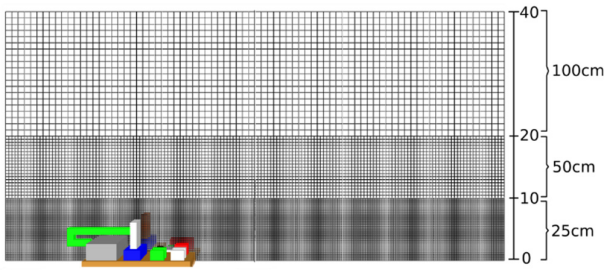

Figure 13: Computational domain and the numerical mesh used in the simulations. Inner values are in metres and outer values represent the computational cell size in centimetres.

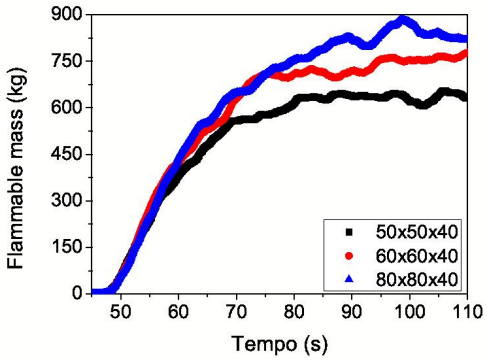

Figure 14: Growth of the flammable material for three different computational domains (50.0 m long x 50.0 m wide x 40.0 m in height), (60.0 m long x 60.0 m wide x 40.0 m in height) and (80.0 m long x 80.0 m wide x 40.0 m in height).

Figure 15 presents the results with the updated computational domains. Analysis of Figure 15 shows no significant difference between the results obtained for the selected computational domains.

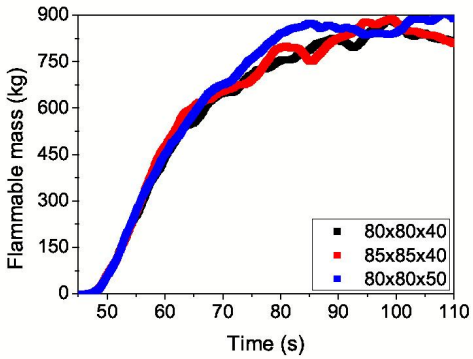

Figure 15: Development of the flammable cloud in the three different computational domains (80.0 m long x 80.0 m wide x 40.0 m in height), (85.0 m long x 85.0 m wide x 40.0 m in height) and (80.0 m long x 80.0 m wide x 50.0 m in height).

DESQr-FDS vs. ANSYS CFX

The DESQr formulation was applied to specify the new boundary condition based on the assumption of incompressible flow for Mach number below 0.30.

The numerical findings are compared with the results obtained using ANSYS-CFX.

Figure 16 below shows the geometry considered in the simulations. All together, 4 wind directions were considered (wind blowing from North, South, East and West). The leak was placed at the centre of the process deck pointing downwards (negative z).

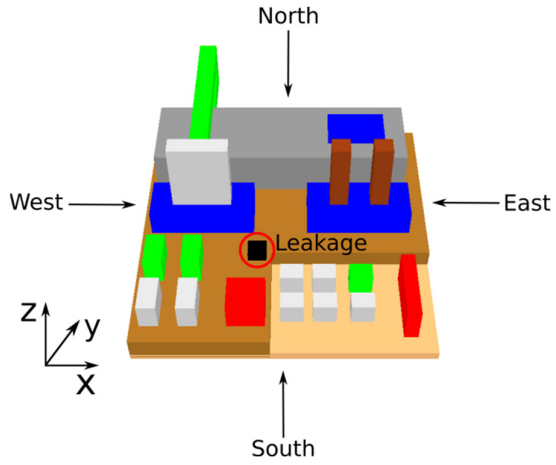

Figure 16: Geometrical model of the chemical process area considered in the computational analysis. The gas leak is placed at the centre of the area. Black arrows indicate the wind directions considered in the gas dispersion analysis.

Boundary conditions for wind modelling in the gas release were set at the prescribed velocity at the inlet and zero gradient for variables in the flow direction at the outlet. Methane was set as the pure substance. Structures and the ground deck were treated as a wall/solid boundary. Table 1 describes the boundary conditions used for this case. An orifice size of 0.9 m and a velocity released of 100 m/s, resulting in a mass flow rate of 53.43 kg/s, was investigated as suggested by Lewis *et al*. (2000).

The key parameters of the simulation are listed in Table 2 for both codes. The ANSYS-CFX setup was based on Ferreira *et al*. (2014).

Table 1: Set of boundary conditions applied in DESQr-FDS and ANSYS CFX.

Boundary conditions	DESQr-FDS	ANSYS-CFX
Wind inlet (m/s)	2.0	2.0
Gas inlet (m/s)	100	100
Gas concentration (vol/vol)	1	1
Orifice size (m)	0.9	0.9
Wind outlet (m/s)	open	open
Structures and ground	wall	wall

Table 2: Simulation parameters used in DESQr-FDS and ANSYS CFX for gas dispersion analysis in the process deck.

Simulation parameters	DESQr-FDS	ANSYS-CFX
Flow condition	Transient	Stationary
Flow regime	Subsonic	Subsonic
Flow type	Incompressible	Incompressible
Heat transfer	Isotherm	Isotherm
Turbulence resolution	LES	RANS
Turbulence model	Dynamic Smagorinsky	$k-\epsilon$
Discretization method	Upwind	Upwind

Figure 17, Figure 18, Figure 19 and Figure 20 show the slice cut (2.5 metres above the process deck) for methane concentration transported by the wind blowing from the north, south, east and west. All Figures presented below show a similar gas cloud contour. In all cases the gas leak is pointing downwards and the gas pattern follows the wind direction.

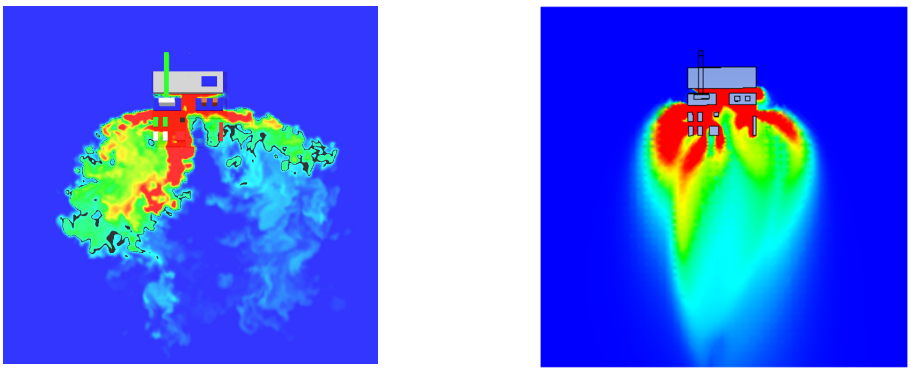

(a) (b)

Figure 17: Top view of methane dispersion transported by the wind blowing from the north. (a) DESQr-FDS code. (b) ANSYS-CFX code. Different turbulent length scales are well captured in the LES formulation while the RANS approach relies on average values for gas concentration.

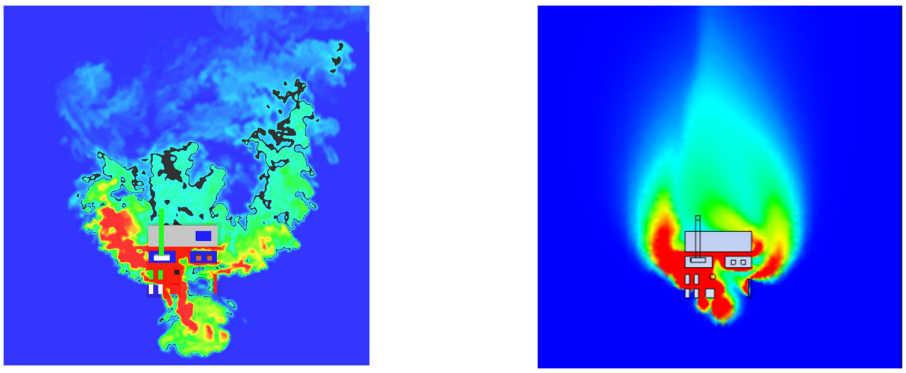

(a) (b)

Figure 18: Top view of methane dispersion transported by the wind blowing from the south. (a) DESQr-FDS code. (b) ANSYS-CFX code. Different turbulent length scales are well captured in the LES formulation while the RANS approach relies on average values for gas concentration.

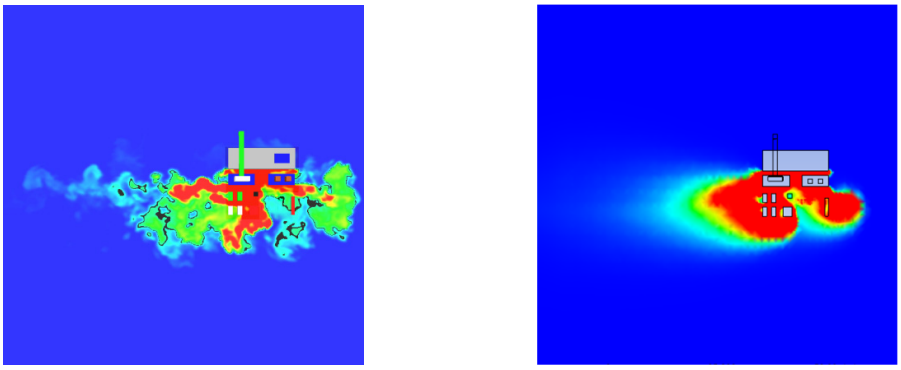

(a) (b)

Figure 19: Top view of methane dispersion transported by the wind blowing from the east. (a) DESQr-FDS code. (b) ANSYS-CFX code. Different turbulent length scales are well captured in the LES formulation while the RANS approach relies on average values for gas concentration.

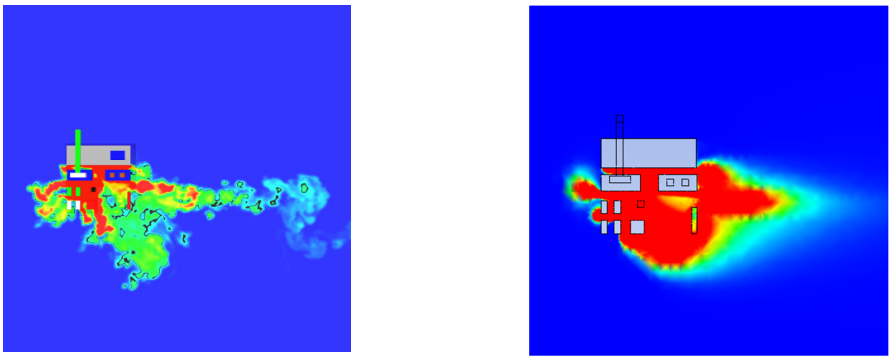

(a) (b)

Figure 20: Top view of methane dispersion transported by the wind blowing from the west. (a) DESQr-FDS code. (b) ANSYS-CFX code. Different turbulent length scales are well captured in the LES formulation while the RANS approach relies on average values for gas concentration.

Analysis of Figure 17(a), Figure 18(a), Figure 19(a) and Figure 20(a) shows the wrinkling of the cloud caused by the different scales of the turbulence represented by the various eddies. On the other hand, Figure 17(b), Figure 18(b), Figure 19(b) and Figure 21(b) show a smooth gas concentration as is expected from the RANS approach.

Figure 21 shows the development of the flammable volume for each simulation. Black dots represent the growth of the flammable volume with time until it reaches the steady-state condition. Red dots represent the volume of the flammable cloud calculated by ANSYS-CFX. The latter was run in steady-state mode in order to reduce the computational time.

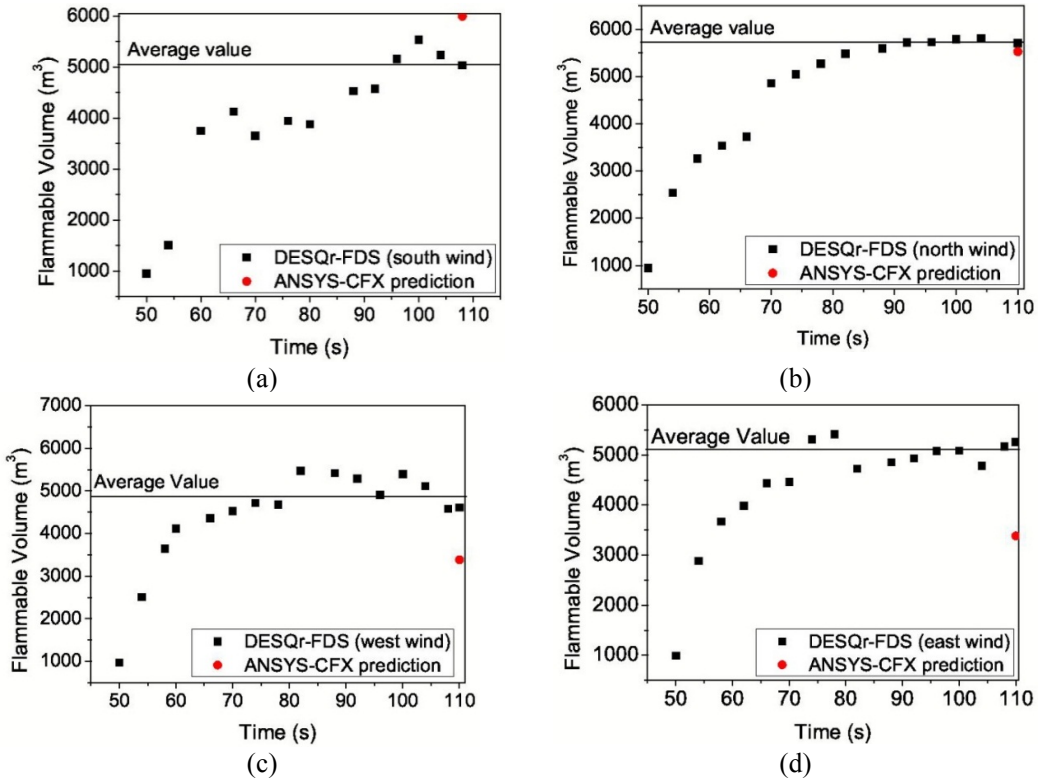

Figure 21: Flammable cloud results for DESQr-FDS and ANSYS-CFX. Results from DESQr – FDS are shown as black dots and they do vary over time. Red dots represent the steady state solution for ANSYS-CFX. Simulations were performed with wind blowing from the (a) north, (b) south, (c) west and (d) east.

Figure 21(a) and Figure 21(b) show the flammable volume value predicted by DESQr-FDS and ANSYS-CFX code considering the wind blowing from the north and south, respectively. Figure 21(c) and Figure 21(d) show the flammable volume value predicted by DESQr-FDS and ANSYS-CFX considering the wind blowing from west and east, respectively. Analysis of Figure 21 shows very little difference between the numerical findings from DESQr-FDS and ANSYS-CFX.

The wind blowing from the north generates a different pattern on the main deck, mainly due to the bluff body effect caused by the accommodation module. Separation of the boundary layer creates a negative pressure gradient in the wake of the flow. As a consequence, the flow is reversed, creating a circulation zone right behind the accommodation module that traps the gas in the platform process area. On the other hand, the symmetry plan observed when the wind is blowing from the west and east does not lead to significant differences in the cloud volume as the ventilation in the platform is quite similar. This is a well known phenomenon in flows around large obstacles and it serves as another positive indication of the performance of DESQr-FDS.

CONCLUSION

A novel jet model, namely DESQr (Diameter of Equivalent Simulation for Quick Run) is proposed. The model was implemented in the framework of FDS (Fire Dynamics Simulator), an open source CFD computational code developed for fire modelling. The turbulence phenomenon is tackled via LES (Large Eddy Simulation).

Originally, FDS was designed for low momentum flows, commonly found in fire scenarios and therefore was not able to handle jet modelling. The code was modified in accordance with the modelling discussed in the DESQr formulation.

Numerical findings were compared with experimental data for gas leaks. The velocity decay profile along the jet centreline was compared with experimental data and good agreement was observed. The results were also compared with a well established commercial CFD code and the same level of accuracy was obtained.

Numerical findings from gas dispersion scenarios considering one leak direction and four wind directions were performed. The results were compared

with ANSYS-CFX and good agreement was observed. Due to more sophisticate modelling of turbulence, DESQr – FDS was able to capture the turbulent eddies in the simulation, which was not possible with the RANS (Reynolds Averaged Navier Stokes) approach used in ANSYS – CFX.

It is therefore suggested to conduct future investigations using LES modelling in ANSYS CFX in order to verify how the open source tool proposed in this work compares with a commercial tool using the same approach for turbulence closure. It is also worth investigating the gas concentration profile along the the jet centreline to verify the level of mixing and air entrainment in the jet. Reynolds stress and Reynolds residual could be calculated using the velocity signal from LES modelling and the results could be compared with available experimental data. It would certainly shed light on the advanced numerical modelling of turbulent jet flows.

NOMENCLATURE

C_e	air entrainment coefficient
D	diameter (m)
D_M	modelled diameter (m)
m	mass flow rate (kg/s)
P	pressure (Pa)
R	universal gas constant (J/K mol)
T	temperature (K)
V	velocity (m/s)
z	downstream distance (m)

Subscript Symbols

a	atmospheric
e	exit condition
eq	equivalent
v	stagnation condition

Greek Symbols

ρ	density
Φ	dependent variable
γ	heat capacity ratio

ACKNOWLEDGEMENT

The authors would like to thank CAPES for the scholarship. Thanks are also due to University of Campinas – FAEPEX and Dr. Emanuele Gissi from the Italian National Fire Service.

REFERENCES

Benintendi, R., Turbulent jet modelling for hazardous area classification. J. Loss Prev. Proc. Ind., 23, 373-378 (2010).

Benintendi, R., Laminar jet modelling for hazardous area classification. J. Loss Prev. Proc. Ind., 24, 123-130 (2011).

Birch, A. D., Hughes, D. J., Swaeld, F., Velocity decay of high pressure jets. Comb. Sci. Tech., 52(1-3), 161-171 (1987).

Dejoan, A., Santiago, J. L., Pinelli, A., Martilli, A., Comparison between LES and RANS computations for the study of contaminant dispersion in the MUST field experiment. Seventh Symposium on the Urban Environment (2007).

Ferreira Jr., E. S., Vianna, S. S. V., A novel and free large eddy simulation tool for gas dispersion. Int. J. Mod. Sim. Petro. Ind., 8, 1-6 (2014).

Ferreira, T. D., Vianna, S. S. V., A novel coupled response surface for flammable gas cloud volume prediction. Int. J. Mod. Sim. Petro. Ind., 8, 7-16 (2014).

Galeev, A. D., Starovoytova, E. V., Ponikarov, S. I., Numerical simulation of the consequences of liquified ammonia instantaneous release using FLUENT software. Proc. Saf. Env. Prot., 91(3), 191-201 (2013).

Germano, M., Piomelli, U., Moin, P., Cabot, W. H., A dynamic sub-grid scale eddy viscosity model. Phys. Fluids, A3, 1760-1765 (1991).

Hussain, A. K. M. F., Zaman, K. B. M. Q., The preferred mode of the axisymmetric jet. J. Fluid Mech., 110, 39-71, (1981).

Lewis, M. J., Lea, C. J., Health safety laboratory. A study of the consequences of leaks from gas turbine power plant sited in a turbine hall. Fire and Explosion (2000).

Mannan, S., Emission and Dispersion. Lees' Loss Prevention in the Process Industries. Butterworth-Heinemann, Oxford, 4th Ed., 752-1074, (2012).

McGrattan, K., Hostikka, S., McDermott, R., Floyd, J., Weinschenk, C., Overholt, K., Fire Dynamics Simulator, User's Guide. NIST Special Publication, v. 4 (2014).

Mouilleau, Y., Champassith, A., CFD simulations of atmospheric gas dispersion using the Fire Dynamics Simulator (FDS). J. Loss Prev. Proc. Ind., 22, 316-323 (2009).

Ricou, F. P., Spalding, B., Measurements of entrainment by axisymmetric turbulent jets. J. Fluid Mech., 11, 21-32 (1961).

Ryder, N. L., Sutula, J. A., Schemel, C. F, Hamer, A. J., Brunt, V. V., Consequence modeling using the

fire dynamics simulator. J. Haz. Mat., 115(1-3, 11), 149-154 (2004).

Scargiali, F., Di Rienzo, E., Ciofalo, M., Grisafi, F., Brucato A., Heavy gas dispersion modelling over a topographically complex mesoscale: A CFD based approach Proc. Saf. Env. Prot., 83(3), 242-256 (2005).

Tauseef, S. M., Rashtchian, D., Abbasi, S. A., CFD-based simulation of dense gas dispersion in presence of obstacles. J. Loss Prev. Proc. Ind., 24(4), 371-376 (2011).

Wakes, S. J., High aspect ratio orifice jet leaks within a production area of an offshore superstructure. Third International Conference on CFD in the Minerals and Process Industries - Melbourne, 32 (2003).

Witlox, H. W. M., Harper, M., Oke, A., Stene, J., Validation of discharge and atmospheric dispersion for unpressurised and pressurised carbon dioxide releases. Proc. Saf. Env. Prot., 92(1), 3-16 (2014).